WEIGH-IN-MOTION STUDIES AT PTI: PRELIMINARY RESULTS

Ümit Sönmez[1], Donald Streit[2], Robin Tallon[2], David Klinikowski[2]

[1]MEKAR Laboratory, Mechanical Engineering Department, Istanbul Technical University, Gümüşşuyu, Istanbul, TÜRKİYE
[2]Pennsylvania Transportation Institute, The Pennsylvania State University, University Park, Pennsylvania, USA

Ümit Sönmez , corresponding author
[1]MEKAR Laboratory, Mechanical Engineering Department, Istanbul Technical University, Gümüşşuyu, Istanbul, TÜRKİYE
Phone: (90)-212-293-1300 Extension:2435
E-mail address: usonitu@gmail.com

ABSTRACT

The various conditions of dynamic vehicle tire forces on pavement loading have been investigated by using strip-type, commercially-available piezo-electric Weigh-In-Motion (WIM) sensors. Two rows of four strip-type sensors were installed at a distance of 4.1 m apart. Tests were performed using a two axle vehicle under three different loading conditions (empty, half load and full load), four vehicle speeds, and three tire pressures. The test vehicle drove over the WIM installation five times for each particular condition.

Typically, WIM load is found by empirically relating the peak voltage of the signal to the static wheel weight and the area under the signal, while speed is not considered. In the case of the strip-type sensors, only a part of the tire patch is in contact with the sensor at a given time; therefore, it is necessary to integrate the sensor response over the tire patch to find the WIM load. A formula considering the area under the recorded WIM signal and the moving load is presented herein.

Another purpose of this preliminary study was to determine whether static calibration factors of strip-type sensors are sufficient to calculate the vehicle dynamic load. During this study, the WIM system was not dynamically calibrated; instead, very accurate, static factory and field calibration factors were used.

WEIGH-IN-MOTION STUDIES AT PTI:
PRELIMINARY RESULTS

Ümit Sönmez[1], Donald Streit[2], Robin Tallon[2], David Klinikowski[2]

[1]MEKAR Laboratory, Mechanical Engineering Department, Istanbul Technical University,
Gümüşşuyu, Istanbul, TÜRKİYE
[2]Pennsylvania Transportation Institute, The Pennsylvania State University,
University Park, Pennsylvania, USA

1. INTRODUCTION

Weigh-In-Motion (WIM) technique has been used by most states to obtain truck axle weights while the vehicle is in motion (dynamic weight) in an expedient and comprehensive method. However, the challenge is to accurately relate those measurements to the static weight of the vehicle. This is because pavement profile and roughness combined with the suspension system of the moving truck introduce instantaneous changes in force applied to the pavement above and below the static weight of the truck. It would be a coincidence if the static weight measurement and the dynamic weight reading of a WIM strip were the same. In fact, WIM devices often do not record the same weight under the same measurement parameters (Mamlouk, 1997). In other words, WIM devices do not duplicate the static weight, which is a great concern among highway engineers. In the study reported herein, well-proven WIM sensor static calibration factors are used to calculate the pavement load (Sönmez et al., 2000).

Road-mounted WIM sensors are typically used to calculate vehicle axle and vehicle gross static weight. In order to do this, so-called dynamic calibration factors are found by minimizing the difference between the mean of several dynamic wheel/axle load measurement passes and the measured static wheel/axle load. These dynamically-calibrated WIM systems behave well within the range of load in which they were calibrated; however, they tend to measure less than static weight for the lighter loads and more than static weight for the heavier loads (Barbour, I.A., and Newton, 1992).

Another approach evolved wherein sets or series of sensors were used to calculate vehicle loads. Cebon (1989) performed theoretical analysis and concluded that a WIM device with three evenly-spaced sensors could provide a reasonable estimate of the static load for a wide range of speeds and dynamic loading frequencies. Later, Cole et al. (1992) developed a portable mat consisting of strip sensors installed at 0.4-m intervals to investigate heavy vehicle highway loads. The mat was calibrated using slow moving vehicles and the accuracy was confirmed using an instrumented vehicle. In the study presented herein, the effects of vehicle load, speed, and tire pressure on pavement loads are investigated using strip-type WIM sensors installed flush with the surface of the road. A new, accurate, and precise concept of how WIM signals should be analyzed and how the WIM load should be calculated is presented in this research.

2. WIM INSTALLATION AND WIM SIGNAL

The WIM installation at the Pennsylvania Transportation Institute's (PTI's) test track facility consists of two rows of strip-type, piezo-electric sensors installed at a distance of 4.1 m apart. A schematic of the configuration is shown in figure 1. According to Barbour and Newton (1992), the optimum distance between the two rows of sensor is 4 m apart. Underground wiring to a roadside equipment cabinet housing the system instrumentation completes the installation.
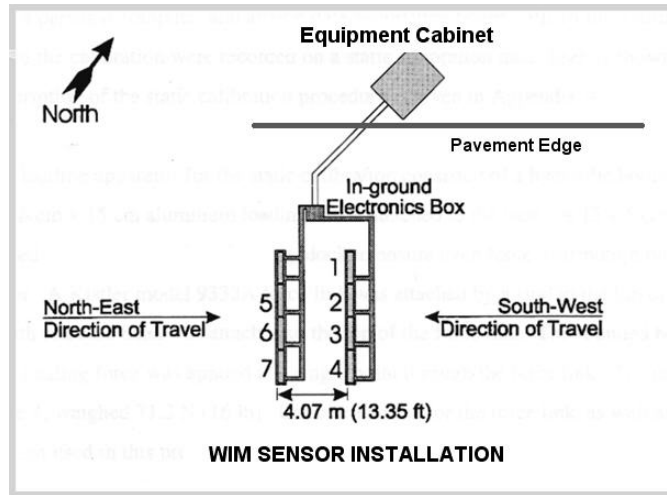
Figure 1: Schematic of the WIM installation at PTI's test track.

An example of the WIM signal data collected from sensor two is plotted in Figure 2. This plot represents a three-axle, heavy vehicle rolling over one of the strip sensors at 56 km/h. The three peaks correspond to the left front (steering), left middle (forward rear) and left, rear-most wheels of a heavy-duty vehicle. In an effort to show the clarity of the WIM signal, the third peak of Figure 2 is enlarged and shown in Figure 3.
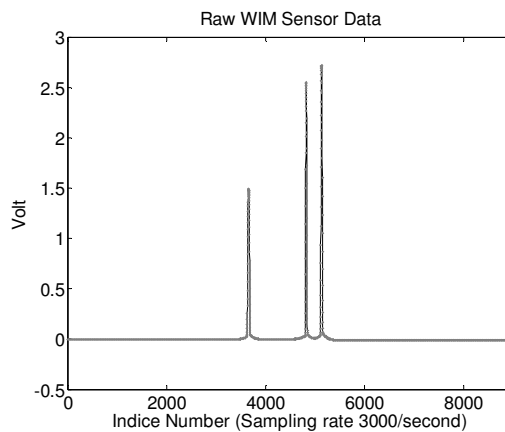

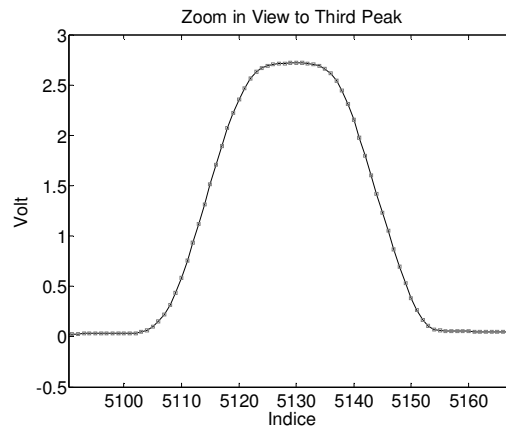**Figure 2: Typical WIM sensor response to a three-axle truck.**

Figure 3: Enlarged view of third peak of the WIM sensor response.

The strip-type WIM sensor used in this study consists of twenty individual piezoelectric load cells contained in a 5 cm by 100 cm strip. The load cells are connected with each other in a parallel circuit that behaves as one sensor unit. Twelve-channel amplifiers were used to record the WIM signal as the vehicle passes over the WIM sensors. These amplifiers have a set gain; therefore, prior to data measurement, the amplifier gain for each channel was adjusted according to the experiment need and recorded. The WIM data was collected by a portable personnel computer with a 16-bit analog data acquisition board installed. Data from eight WIM sensors were recorded at a sampling rate of 2,500 samples per second during the test runs. Up to six seconds of data were recorded for each test run, depending on the vehicle speed and hand triggering time, resulting in matrices with dimensions of 15,000 by 8. MATLAB routines were written to process the raw data of the WIM experiments and to automate the data processing stage.

A two-axle test vehicle was used during the dynamic testing. This vehicle was a pickup truck with dual rear wheels that had a gross vehicle rating of 44,480 N. The test vehicle was weighed before the experiments using digital scales with an accuracy of 89 N.

3. WIM LOADING

The mathematical formulation of the WIM load calculation scheme for strip-type sensors (sensors having a smaller surface area than the tire patch) is derived in this section. The mean dynamic axle loads and the mean dynamic gross vehicle load calculations are then presented.

3.1 Mathematical Derivation of Load Calculation Scheme

Consider the one-dimensional, vertically-distributed load rolling over a strip-type WIM sensor at a constant speed as shown in Fig. 4.
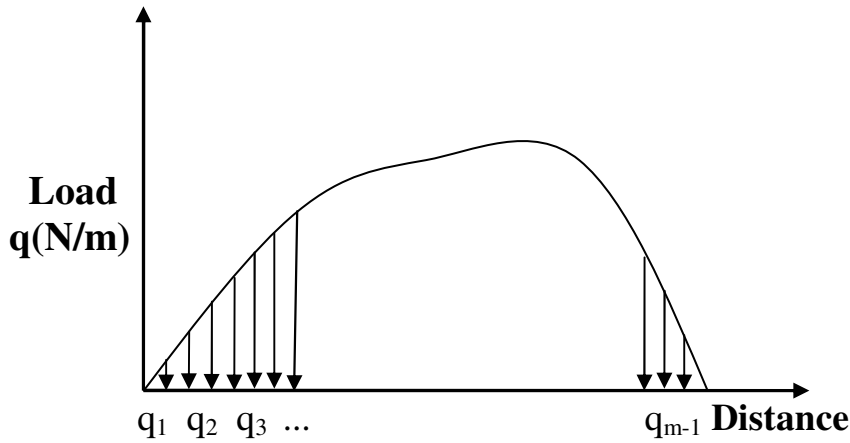
Figure 4: Vertically-distributed load.

The resulting vertical force F of the distributed load exerted on the surface is given by:

$$F = \int_0^l q(x)dx \qquad (1)$$

where l is the length of the applied load, and $q(x)$ is the one-dimensional load distribution function (N/m). Let's assume the sensor reading is sampled at every Δt, time interval, and the distributed load is moving Δx, distance, in each sample time creating a discrete signal representation of the one-dimensional, applied load. Using the trapezoidal integration scheme F may be calculated as:

$$F = \sum_{i=1}^m (q_i + q_{i+1})\Delta x / 2 \qquad (2)$$

Consider the wheel moving towards a strip-type WIM sensor, as shown in Figure 5, where w, the sensor width, is $n\Delta x$, and L the load length or tire patch, is $m\Delta x$. Let's assume n and m are integer numbers for the simplicity of the derivation.
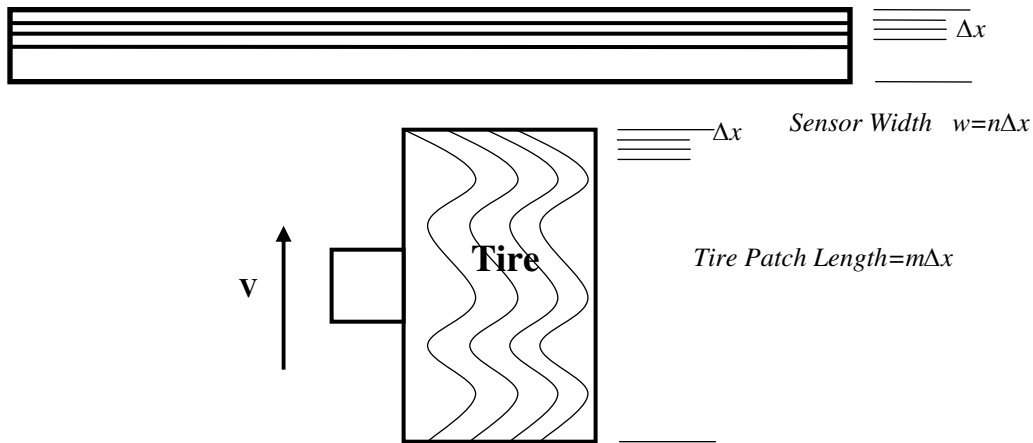

Figure 5: Schematic of wheel rolling toward the WIM sensor at a constant speed.

The WIM sensor reading is recorded at regular intervals $\Delta t = 1/samplingrate$, as the wheel moves over the sensor at a constant speed (see Figure 6).

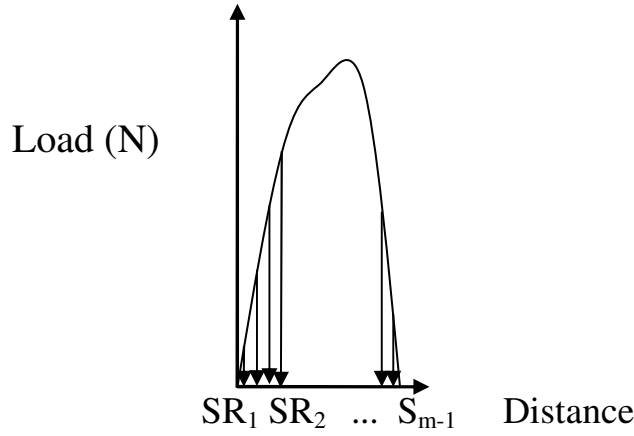**Load (N)**

SR₁ SR₂ ... Sₘ₋₁ Distance

Figure 6: Road based sensor reading versus distance plot.

Data recorded in this manner corresponds to the resulting load on the sensor, as given by the following equations:

$$SR_1 = q_1\, \Delta x/2$$
$$SR_2 = q_1\, \Delta x/2 + (q_1 + q_2)\Delta x/2$$

.

$$SR_n = \sum_{i=1}^{n}(q_i + q_{i+1})\Delta x/2 \tag{3}$$

.

$$SR_p = \sum_{i=p}^{p+n}(q_i + q_{i+1})\Delta x/2$$

...

The area under the sensor's measured reading, load, and the distance plot, A_{ALDP}, may be calculated as:

$$A_{ALDP} = \sum_{i=1}^{m}(SR_i + SR_{i+1})\Delta x/2 \tag{4}$$

Equation 2, Equation 3, and Equation 4 are used to obtain Equation 5. Equation 5 shows that the area of the plot under the sensor's measured response (the load) and the distance axis (the time axis mapped to distance axis assuming constant wheel velocity) is proportional to the width of the sensor traversed and the total vertical load exerted on the road surface.

$$A_{ALDP} = n\Delta x * \sum_{i=1}^{m}(q_i + q_{i+1})\Delta x/2 = w*F \tag{5}$$

Where A_{ALDP} is the area under the load and the distance curve obtained from the WIM reading, w is the traversed width of the sensor, and F is the total vertical load applied to the road by the wheel.

3.2 WIM Load Calculation Scheme

Typically WIM load is found by empirically relating the peak voltage of the signal to the static wheel weight; while the area under the recorded signal and the speed are not considered. In the case of the strip-type sensors, the tire patch is larger than the sensor width. This results in a condition where, for a given time, only a part of the tire patch area is in contact with the sensor area. Therefore, it is necessary to integrate the sensor response over the tire patch to find the wheel load, as given in Equation 6.

$$TireForce = \frac{\left(Gain * SCF * \sum V_i (i * axle_{vel}) - V_0\right)}{Sensorwidth * Samplingrate} \qquad (6)$$

In Equation 6, V_i is the i-th voltage reading from the WIM sensor, V_o is the voltage bias or offset, and SCF is the sensor static calibration factor. The vehicle velocity (axle velocity) calculation was based on the known distance between WIM sensor rows and the time lapse between the two WIM sensor responses.

Dynamic tire forces were first calculated individually at each sensor location. The two front and the two rear tire forces were combined to find the corresponding front and rear axle loads, respectively. Then, the axle loads were averaged over the sensor rows to find the mean axle load.

4. TESTING PROCEDURE AND WIM RESULTS

The dynamic testing procedure is summarized and WIM testing results are presented in this section.

Static wheel load measurements were performed on each of the WIM sensors. The static weight on the vehicle wheels was measured with portable digital scales at the WIM site and in the garage. After determining that no change in measured weight occurred as a result of performing the measurements in the different locations, all static measurements were performed in the garage. Three loading conditions were investigated; the truck with no load (empty condition), the truck loaded with ballast to approximately half of its maximum payload (half-loaded condition), and the truck loaded to approximately its maximum payload condition (fully-loaded condition). The static wheel weights are given in Table 1.

Table 1: The static wheel loads measured.

	Front Left Wheel (kg)	Front Right Wheel (kg)	Rear Left Wheel (kg)	Rear Right Wheel (kg)
Empty Condition	825	780	807	762
Half-Loaded Condition	889	844	1107	1152
Fully-Loaded Condition: Nominal Tire Pressure	789	871	1478	1560
Fully-Loaded Condition: +30% Tire Pressure	789	844	1415	1533
Fully-Loaded Condition: -30% Tire Pressure	762	780	1596	1551

The first testing sequence consisted of the empty vehicle being driven over the WIM sensors for a total of twenty passes. Five test runs were performed at each of four target speeds (8 km/h, 24 km/h, 56km/h and 80km/h). For the second testing sequence, the half-loaded test vehicle was used to perform the same test procedure, five passes at four speeds. The fully-loaded test sequence included an additional parameter—tire pressure. The previously-described procedure was repeated at each of three tire pressure conditions: -30% of manufacturer's rated pressure, at manufacturer's rated pressure, and +30 % of manufacturer's rated pressure, for a total of 100 runs.

The test vehicle's front and rear axle loads and the gross vehicle load were obtained from the WIM sensors through the procedure explained in section 3. First, the WIM axle loads were divided to static axle loads and the ratios and corresponding standard deviations were plotted. Even if the WIM sensors accurately read the dynamic loads, the calculated ratios (WIM load/static load) would have fluctuated around 1.0 due to vehicle dynamics alone. The error plots showed a standard deviation of the calculated mean axle and gross vehicle loads on subsequent runs. This data provided a measurement of the WIM sensor's repeatability.

The processed results for the empty test condition are shown in Figure 7. The vehicle's front axle weight from static load measurement was slightly higher than the static rear axle weight; however, the vehicle's dynamic rear axle load was 10 % to 20 % higher than the dynamic front axle load. The vehicle's dynamic front axle load displayed a downward trend as the test speed increased, as can be seen in Figure 7. The fourth (highest) test speed showed the lowest load factor (~1.0). The third test speed for the vehicle's rear axle load showed the highest load factor (~1.25), demonstrating an increasing trend followed by a decrease at the highest speed. The gross dynamic load factor was between 1.10 and 1.20 indicating no significant change related to speed. The highest deviation in load readings was at the lowest test speed.
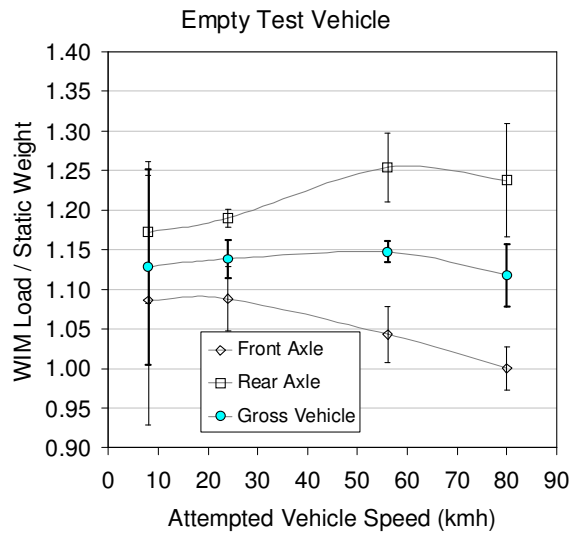
Figure 7. Plot of WIM loads in the empty condition.

The general trend of the WIM results for the half-loaded condition of the vehicle (see Figure 8) was significantly different from the other two loading conditions. The rear axle was at its maximum dynamic load while traversing the WIM sensors at 8 km/h and the load consistently decreased as the vehicle speed increased. The front axle load showed an increase between the first and second test speeds, followed by a decrease between the remaining speeds. Comparing the parabolic distribution of the test results, it is suspected that the vehicle's axle dynamics at 8 km/h were the primary cause of this unusual trend. In the half-loaded condition, the gross dynamic load factor decreased from 1.28 to 1.05; thereby indicating a significant change with relative to test speed. The highest deviation in load readings was at the lowest speed.
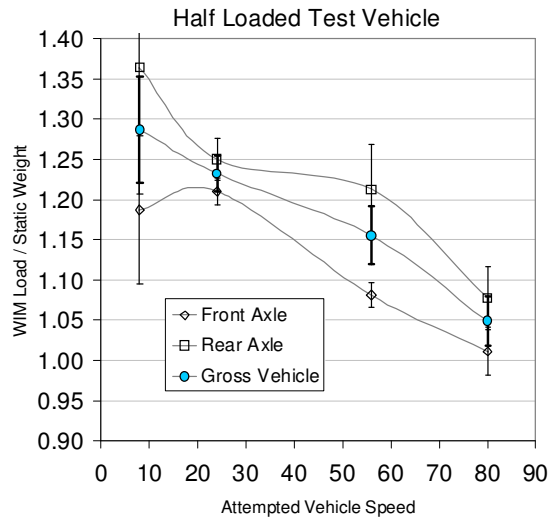

Figure 8: Plot of WIM loads in the half-loaded condition.

Lower tire pressures filter the input to a spring suspension, thereby attenuating the wheel mode contribution to the tire force. Lowering the tire pressure also creates a larger tire-pavement contact area, thereby reducing the stresses and strains at any given point on the pavement. Because tire pressure has an effect on vehicle dynamics, tests were performed in the fully-loaded condition at three different tire pressures. The WIM results corresponding to

the fully-loaded conditions are presented in Figures 9, 10 and 11. The same parabolic trend can be seen in the gross dynamic vehicle load factor of the three tire pressure conditions, suggesting a minor affect of the tire pressure on the WIM load readings.
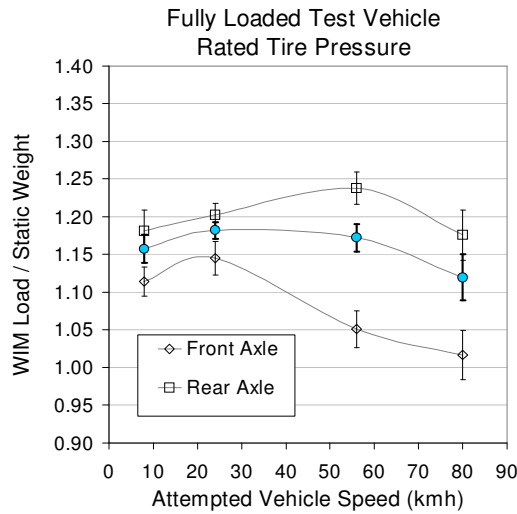

Figure 9: Plot of WIM loads for fully-loaded condition (rated tire pressure).
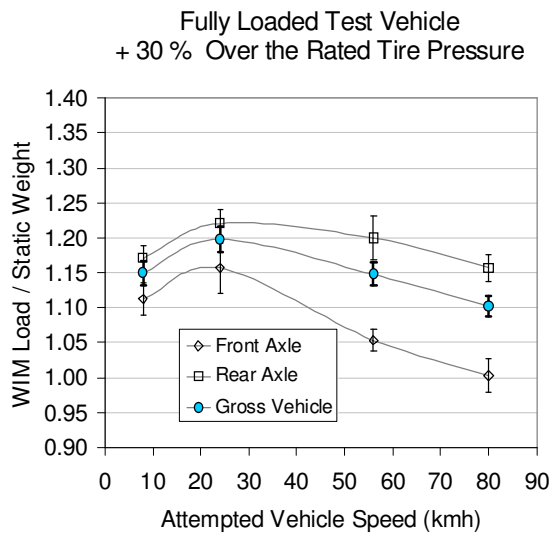

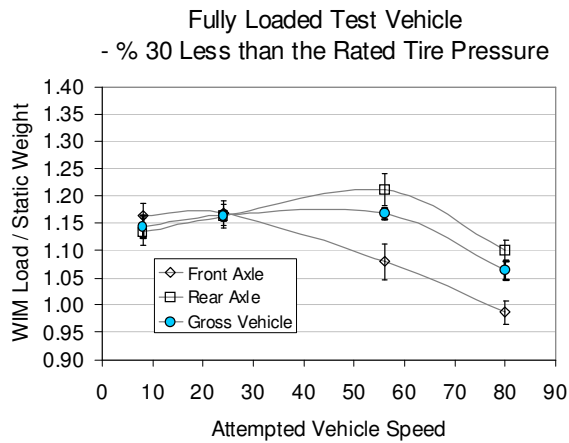**Figure 10: Plot of WIM loads in fully-loaded condition (+ 30 % tire pressure).**

Figure 11: Plot of WIM loads at fully-loaded condition (- 30 % tire pressure).

The rear axle load factor reached a maximum at the third speed (~1.23) and a minumum at the first (lowest) and fourth (highest) speeds for the fully-loaded condition at the manufacturer's rated tire presure (See figure 9). The rear axle load factor was higher than the front axle load factor at all speeds. Under the same loading and tire pressure conditions, the maximum front axle load factor was at the second speed (~1.15) and was the lowest at the fourth speed. The gross vehicle load factors were between the 1.10 to 1.20 range. The highest deviation was found at the fourth speed.

For the fully-loaded condition with the +30 % tire pressure parameter, trends similar to the rated tire pressure condition were observed. The gross vehicle load factors were 1.10 to 1.20, indicating no significant deviation relative to speed.

The following observations are made for the fully-loaded condition with the - 30 % tire pressure parameter. Although the gross dynamic vehicle loads show trends similar to the other two fully-loaded conditions, there is a noteworthy difference in the dynamics of the axle loads at the first two speeds. Unlike the first two fully-loaded conditions (rated and +30% tire pressure), the front axle load factor and the rear axle load factor are close to each other at the first two test speeds. In fact, the front axle load factor is higher than the rear axle load factor at the first speed. This phenomenon is due to the decreased stiffness of the tires. The front axle load factor reaches a maximum at the first (lowest) speed and its lowest at the fourth speed. The gross vehicle load factor is 1.05 to 1.20, again indicating that there is no significant deviation between speeds.

5. DISCUSSION

It is interesting to note that data from this study shows the standard deviation of the WIM system performance is less for the gross vehicle load than it is for the individual axle loads. This observation demonstrates that the calculation of the gross vehicle load would result in smaller variations than the calculation of individual axle loads.

Gross vehicle load data from the 8 km/h tests shows a larger standard deviation than any other speed. The researchers feel that this is due to speed variations as the vehicle passes over the WIM sensor. When traveling at 8 km/h, the vehicle will spend more time on the WIM sensor than when traveling at 80 km/h; and, therefore, deviations in speed will have more of an impact on the calculations.

As the vehicle speed progress from 8 to 24 km/h, from 24 to 56 km/h, and from 56 to 80 km/h, the mean values of gross vehicle load data increases first, then decreases until they reach a minimum value of 1.05-1.12 at 80 km/h. This particular parabolic behavior is believed to be the result of the test vehicle dynamics and is observed in most of the tests. However it is necessary to run a vehicle simulation corresponding to the half vehicle model of skid truck on the measured road profile of PTI test track in the vicinity of WIM sensors to confirm this conclusion.

6. CONCLUSIONS

The strip-type WIM sensor system had a tendency to indicate dynamic load at 5% to 15% higher than the static gross vehicle weight of the test vehicle. This observation suggests that further study of the sensor response relative to dynamic tire load dependence is warranted. Sonmez, et al. (2000) demonstrated that increasing the strip-type sensor load to 5000 N by means of an on-site uniform loading/calibration procedure showed no effect on the WIM sensor's response (i.e., sensor's response was found to be linear).   However, researchers suspect that the dynamic tire loading across the sensor has a load-dependent result due to the introduction of an asymmetric bending moment as the vehicle traverses the sensor. The effect of the bending moment could not be observed in static factory calibration and dynamic field calibrations due to uniform loading, but is suspected present when a tire passes over the WIM sensor.

REFERENCES

1. Barbour, I.A., and Newton, W.H. (1992). Improving the Accuracy of Weigh-In-Motion Systems. *Proceedings of the Third International Symposium on Heavy Vehicle Weights and Dimensions*, pp. 381-386.

2. Cebon D. (August 1989). Design of Multiple-Sensor Weigh-in-Motion Systems. *Proceedings of International Conference on Mechanical Engineering,* part D.

3. Cole D. J., Collop A. C., Potter T.E.C., and Cebon D. (1992). Use of a Force Measuring Mat to Compare the Road Damaging Potential of Heavy Vehicles. *Heavy Vehicles and Roads: Technology, Safety and Policy*, pp. 266-269.

4. Mamlouk M. S. (Nov-Dec 97). General Outlook of Pavement and Vehicle Dynamics. *Journal of Transportation Engineering,* pp. 515-517.

5. Sonmez U., Sverdlova N., Tallon R., Klinikowski D. and Streit D. (2000). Static Calibration Methodology for Weigh-In-Motion Systems. *International Journal of Vehicle Design*, 191-204, Volume 7, Nos 2/3.